Bioorganic Chemistry 82 (2019) 332–339

Contents lists available at ScienceDirect

Bioorganic Chemistry

journal homepage: www.elsevier.com/locate/bioorg

A deuterohemin peptide protects a transgenic *Caenorhabditis elegans* model of Alzheimer's disease by inhibiting $A\beta_{1-42}$ aggregation

Jia Xu, Ye Yuan, Ruining Zhang, Yanhui Song, Tianzhuo Sui, Jiaqi Wang, Chonghan Wang, Yujia Chen, Shuwen Guan, Liping Wang*

School of Life Sciences, Jilin University, Changchun, Jilin, China

ARTICLE INFO

Keywords:
Alzheimer's disease
Deuterohemin peptide
Amyloid β
Caenorhabditis elegans

ABSTRACT

Alzheimer's disease (AD) is a progressive neurodegenerative brain disease and is the most common cause of dementia in the elderly. The main hallmark of AD is the deposition of insoluble amyloid (Aβ) outside the neuron, leading to amyloid plaques and neurofibrillary tangles in the brain. Deuterohemin-Ala-His-Thr-Val-Glu-Lys (DhHP-6), a novel porphyrin-peptide, has both microperoxidase activity and cell permeability. In the present study, DhHP-6 efficiently inhibited the aggregation of Aβ and reduced the β-sheet percentage of Aβ from 89.1% to 78.3%. DhHP-6 has a stronger affinity (K_D = 100 ± 12 μM) for binding with Aβ at Phe^4, Arg^5, Val^{18}, Glu^{11} and Glu^{22}. In addition, DhHP-6 (100 μM) significantly prolonged lifespan, alleviated paralysis and reduced Aβ plaque formation in the $A\beta_{1-42}$ transgenic *Caenorhabditis elegans* CL4176 model of AD. Our results demonstrate that DhHP-6 is a potential drug candidate that efficiently protects a transgenic *C. elegans* model of Alzheimer's disease by inhibiting Aβ aggregation.

1. Introduction

Alzheimer's disease (AD) is the most common age-related neurodegenerative brain disease in those over the age of 65. AD is characterised by the massive deposition of misfolded protein aggregates and neurofibrillary tangles [1], progressive deterioration of memory and cognition, and a gradual worsening of behavioural disturbances [2]. The number of persons with senile dementia is approximately 24 million globally, making AD the fifth leading cause of death in the elderly [3,4]. Gene mutations in Apolipoprotein (Apo) E4, the deposition of tau/amyloid β (Aβ), the region-selective loss of neurons, and changes in hippocampal volume are among the main pathological features of AD [5–7]. The amyloid hypothesis posits that proteolytic cleavage of the amyloid β precursor protein (AβPP) by β- and γ-secretase leads to the production and accumulation of $A\beta_{1-40}$ and $A\beta_{1-42}$ [8,9]. Aβ peptides have the ability to self-assemble into various amyloid species, including intracellular Aβ monomers, highly neurotoxic oligomers (trimers and tetramers), extracellular Aβ protofibrils, fibrils and amyloid deposits. These Aβ species are associated with memory deficits and behavioural dysfunction in humans and AD transgenic mouse models [10–12 13]. Although the causal link between Aβ and AD still remains to be fully clarified, the amyloid hypothesis is supported by numerous lines of evidence [7,14]. There is substantial evidence that the aggregation of Aβ and oxidative stress are interrelated. Aβ overexpression can perturb the oxidant–antioxidant balance *in vivo* [15], and excessive levels of free radicals can cause oxidative damage to proteins, DNA and other molecules [16], resulting in metabolic dysfunction and apoptosis, especially in the brains of AD patients [15]. Accordingly, there has been a great deal of focus on antioxidants and Aβ aggregation inhibitors for alleviating symptoms and slowing the progression of AD.

DhHP-6 is a novel peptide mimetic of microperoxidase-11 (MP-11), which is composed of a deuterohemin (the vinyl groups of oxidised heme) prosthetic group bonded to six amino acid residues (AlaHisThrValGluLys). Deuterohemins are easily occupied by histidine in polypeptides to form pentacoordinate iron-porphyrin complexes, which compose a catalytic site the same as natural MP-11 [17,18]. Both deuterohemin and DhHP-6 were designed and synthesised in our laboratory. In our previous studies, DhHP-6 extended the lifespan of wild type *C. elegans* by 19%, and increased resistance to heat stress (35 °C) and H_2O_2 or paraquat-induced oxidative stress in *C. elegans* [19,20], suggesting that DhHP-6 may have beneficial effects on age-related diseases. This encouraged us to investigate whether DhHP-6 may have potential for alleviating Alzheimer's disease, and to determine its potential mechanism *in vitro* and *in vivo*.

C. elegans is an ideal model organism for drug screening and toxicity evaluation because of its short life cycle and ease of cultivation [21].

* Corresponding author at: No. 2699 Qianjin Street, Changchun 130012, China.
E-mail address: wanglp@jlu.edu.cn (L. Wang).

https://doi.org/10.1016/j.bioorg.2018.10.072
Received 3 September 2018; Received in revised form 27 October 2018; Accepted 31 October 2018
Available online 03 November 2018
0045-2068/

The $A\beta_{1-42}$ transgene expressed in the *C. elegans* CL4176 strain model of AD is based on a plasmid from Chris Link. It has an incorrect N-terminal truncation of a signal peptide that results in accumulation of Aβ, amyloid deposition and progressive paralysis [22,23]. In the present study, we investigated (1) whether DhHP-6 reduces the accumulation of Aβ *in vitro*; (2) whether DhHP-6 binds or changes the spatial conformation of Aβ; and (3) whether DhHP-6 alleviates Aβ-induced toxicity and oxidative damage in *C. elegans*.

2. Materials and methods

2.1. Reagents

DhHP-6 was synthesised by solid phase peptide synthesis (SPPS) in our lab as described previously (Fig. S1) [20]. Thioflavin T (ThT) and hexafluoroisopropanol (HFIP) were purchased from Sigma-Aldrich. Levamisole hydrochloride was purchased from Jilin pharmacy. $A\beta_{1-42}$ and LPFFD were purchased from Meilunbio Co., Ltd (Dalian, China). Paraformaldehyde (4%), Triton X-100, Tricine-SDS-PAGE gels (50% glycerol (w/v)), and phosphate-buffered saline containing 0.05% Tween 20 (PBST) were purchased from Solarbio (Beijing, China).

The *C. elegans* strain CL4176, *smg-1(cc546) I;dvIs27 [myo-3p::A-Beta (1–42)::let-851 3′UTR) + rol-6(su1006)] X*, as well as *Escherichia coli* OP50 were obtained from the *Caenorhabditis* Genetics Center (CGC), University of Minnesota, MN, USA.

2.2. Measurement of Aβ fibrils

Thioflavin T (ThT) was used to visualise stacked β sheets of amyloid fibrils *in vitro* and *in vivo*. Binding enhances the fluorescence intensity at 450 nm (excitation wavelength) and 485 nm (emission wavelength). $A\beta_{1-42}$ monomer was prepared using HFIP. To measure the effects of DhHP-6 on the spontaneous aggregation of Aβ *in vitro,* various concentrations of Aβ and DhHP-6 were mixed with ThT in phosphate buffer (PB; pH 7.4), incubated at 37 °C, and the fluorescence intensity was subsequently measured using a microplate reader (GENIOS, Tecan) [24,25]. Fluorescence images of Aβ aggregates were taken on a fluorescence microscope (Olympus IX51, Japan) and Cell Imaging Multi-Mode Reader (BioTek Cytation 3, USA). In ThT fluorescence staining assays, the plaque-like Aβ disposition in *C. elegans* was measured. Thirty synchronised adult worms were treated with *E. coli* OP50 or DhHP-6 (100 μM) at 25 °C for 4 days, and then anaesthetised with levamisole (5 mM, 3 min) and fixed overnight in 4% paraformaldehyde (Solarbio) in phosphate buffered saline (PBS; pH 7.4) at 4 °C. Worms were then permeabilised in 125 mM Tris buffer (pH 7.4 with 5% β-mercaptoethanol (Meilunbio Co., Ltd.)) and 1% Triton X-100 (Solarbio) for 24 h at 37 °C. Then, samples were washed with PBST (Solarbio) 3 times and stained with 0.125% ThT in 50% ethanol for 20 min, followed by destaining with sequential washes in 50%, 75%, and 90% ethanol. The worms were then transferred onto a 2% agar pad and capped with coverslips [26,27]. Images of ThT stained amyloid plaques were taken with a Confocal Laser Scanning Microscope (FV1000, Olympus) and the ThT fluorescence intensity was measured by Image software (NIH, Bethesda, MD).

2.3. SDS-PAGE and western blot analyses

$A\beta_{1-42}$ (15 μM) mixed with DhHP-6 (0, 5, 10, 15 or 20 μM) was dissolved in 10 mM PB, incubated at 37 °C for 24 h, and thereafter mixed with 2× loading buffer and boiled for 10 min. The samples were electrophoresed on Tricine-SDS-PAGE gels (50% glycerol (w/v), Solarbio) and transferred onto 0.22 μm PVDF membranes (Merck Millipore, Germany). After blocking with 5% (w/v) nonfat milk for 1 h, the membranes were probed with a monoclonal anti-$A\beta_{1-16}$ antibody (6E10, Biolegend, USA), and goat anti-mouse IgG H&L (HRP, Abcam, England). Signals were detected with enhanced chemiluminescence (Thermo Fisher, USA), and grey values were calculated using Image software.

2.4. Transmission electron microscopy (TEM)

$A\beta_{1-42}$ dissolved in HFIP was stored at −20 °C as stocks. $A\beta_{1-42}$ stocks, and Aβ mixed with DhHP-6 were dissolved in deionised water and incubated at 37 °C for 5 days. Then, 10 μL aliquots of the samples were placed onto TEM grids, dried, and viewed using a JEM-2100F microscope with a field emission gun operating at 200 kV.

2.5. Bio-Layer Interferometry (BLI) system

BLIs were examined with an Octet RED96 (ForteBio, USA) using Dip and Read (streptavidin) biosensors to observe and measure the interaction of molecules in real time. $A\beta_{1-42}$ (1 mM) was mixed with biotin (30 mM) in PB buffer (pH 7.4) at 25 °C for 30 min, then excess biotin was removed by dialysis at 4 °C overnight. The $A\beta_{1-42}$ immobilised with biotin served as loading buffer. The composition of running buffer was DhHP-6 or LPFFD dissolved in washing buffer (0.05% Tween 20 and 0.1% bovine serum albumin in PB). The BLI kinetic experiments were performed at a constant flow rate of 30 μL/min, with a running time for DhHP-6 of 50 s, followed by the dissociation phase. The dissociation constant (K_D) was fitted using the 1:1 Langmuir binding model using ForteBio Data Analysis 7.0.

2.6. Circular dichroism (CD) spectroscopy

Pure $A\beta_{1-42}$ (75 μM) was mixed with or without 25 μM DhHP-6 in PB (pH 7.4). CD spectra of the samples were recorded at 25 °C (bandwidth: 1.0 nm; sensitivity: 0.5 nm; scanning speed: 500 nm/min) using a Jasco J-715CD spectropolarimeter. The representative scans were plotted as ellipticity (mdeg) versus wavelength (nm).

2.7. Molecular docking

The 3D structure of DhHP-6 was built using the Chem 3D program. The crystal structure of $A\beta_{1-42}$ was extracted from the Protein Data Bank (PDB ID: 1IYT) [28]. The molecular docking and the structure of DhHP-6 bound to $A\beta_{1-42}$ were generated using AutoDock 3.1 and Discovery Studio (DS) Visualizer 4.0, respectively.

2.8. Lifespan and paralysis assays

Aβ toxicity leads to paralysis and the subsequent death of the transgenic *C. elegans* CL4176 strain. The CL4176 strain was cultured and propagated in NGM (Nematode Growth Medium) seeded with *E. coli* OP50 at 16 °C. Synchronised adult worms (70 per group) were cultured with 100 μM DhHP-6 plus 50 μM 5-fluorouracil at 25 °C to induce Aβ expression. For the lifespan assay, surviving and dead worms were counted daily until all died. For the paralysis assays, the proportion of paralysed individuals failing to complete full body movement but with pharynx contraction were calculated. The survival curve and proportion of paralysed worms were plotted with GraphPad Prism 5 (GraphPad Software, La Jolla, CA). The same culture and treatment protocols were used for all assays in this paper.

2.9. Calculations and statistical analysis

Data were expressed as the mean ± SD, and the standard error of the mean is indicated by a bar in the figures. Statistical analysis was carried out using the log-rank (Mantel-Cox) test and the *t*-test using GraphPad Prism 5 (GraphPad Software). A value of $p < 0.05$ was considered statistically significant.

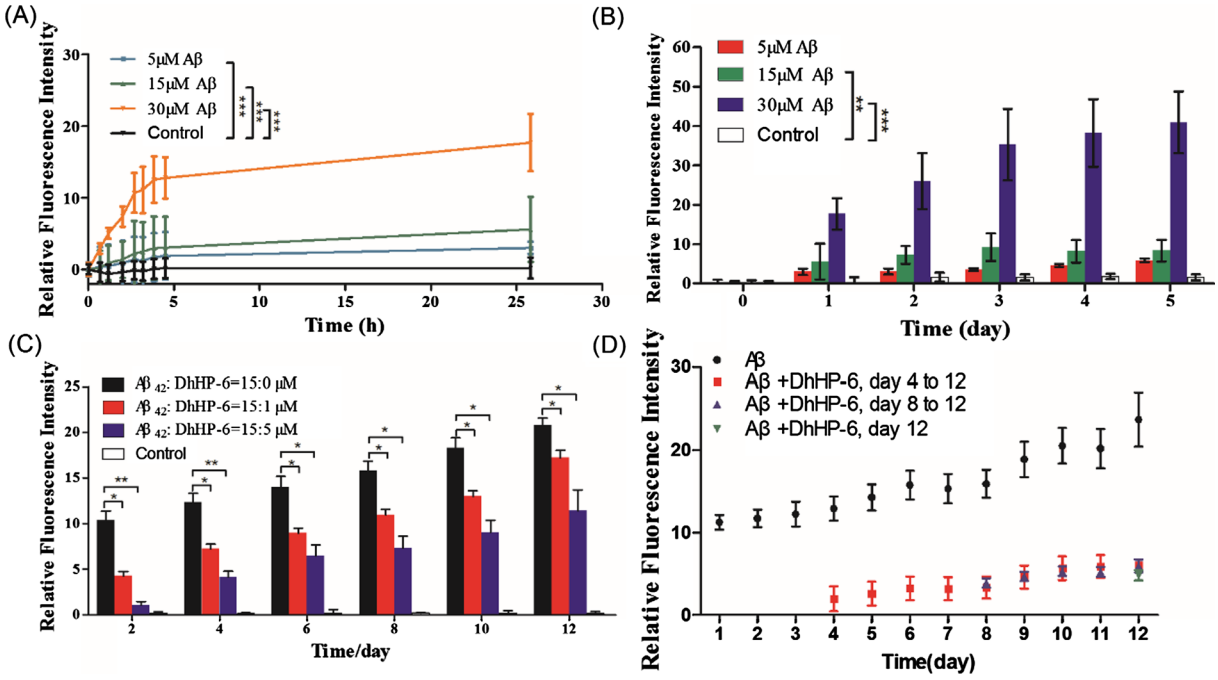

Fig. 1. DhHP-6 effectively reduced the aggregation of $A\beta_{1-42}$ in a dose-dependent manner, as shown by ThT assay. $A\beta_{1-42}$ stocks were dissolved in PB buffer with 5 mM ThT and incubated at 37 °C. Relative fluorescence intensity of Aβ was quantified (A) in the short term (at 30 min intervals, $^{***}p < 0.001$) and (B) in the long term (daily, $^{**}p < 0.01$; $^{***}p < 0.001$). (C) Various concentrations of DhHP-6 on the aggregation of $A\beta_{1-42}$ were tested. $A\beta_{1-42}$ was mixed with DhHP-6 (15:0, 15:1, 15:5 M ratios) and incubated at 37 °C for 12 days. Fluorescence intensity was measured per 2 days ($^{*}p < 0.05$; $^{**}p < 0.01$). (D) DhHP-6 was added at different stages of $A\beta_{1-42}$ fibrillation. The red, blue and green dots represent the relative fluorescence intensity of Aβ after DhHP-6 was added on day 4, 8 and 12, respectively. The error bars represent the average ThT fluorescence intensity values from three consecutive measurements and their corresponding standard deviations.

3. Results

3.1. DhHP-6 inhibits the aggregation of $A\beta_{1-42}$ in vitro

ThT was used to visualise stacked β sheets of amyloid fibrils *in vitro* and *in vivo* [29,30]. The effects of various concentrations of DhHP-6 and co-incubation times on the aggregation of $A\beta_{1-42}$ were tested by ThT assay. Pure $A\beta_{1-42}$ (5 μM, 15 μM, 30 μM) was assessed in the short term (at 30 min intervals, Fig. 1A) and in the long term (daily, Fig. 1B), which indicated that $A\beta_{1-42}$ fibrillogenesis is time-dependent at 37 °C and that 15 μM $A\beta_{1-42}$ is the optimal concentration in ThT assay. $A\beta_{1-42}$ was mixed with DhHP-6 (15:0, 15:1, 15:5 M ratios) and incubated at 37 °C for 12 days (Fig. 1C). DhHP-6 (5 μM) significantly delayed or reduced the self-assembly of β-sheets in a dose-dependent manner. DhHP-6 (5 μM) was added at different stages of $A\beta_{1-42}$ fibrillation, shown in Fig. 1D. The red, blue and green dots represent the relative fluorescence intensity of Aβ after DhHP-6 was added on day 4, 8 and 12, respectively (Fig. 1D). The results indicate that DhHP-6 rapidly inhibited the aggregation of Aβ.

The visual effect of DhHP-6 on $A\beta_{1-42}$ aggregation was also evaluated by fluorescence microscopy and a cell imaging multi-mode reader. The aggregation of $A\beta_{1-42}$ at initial concentrations of 0 to 40 μM were photographed (Fig. 2A). The fluorescence intensity (i.e., aggregation) increased in a dose-dependent manner, with 15 μM $A\beta_{1-42}$ producing the best effect, consistent with the results in Fig. 1. By incubating with DhHP-6, the aggregation of Aβ was significantly decreased (Fig. 2B and C). Together, these findings show that DhHP-6 significantly reduces the aggregation of $A\beta_{1-42}$ *in vitro* in a dose-dependent manner (inhibition of 72.62% by 5 μM DhHP-6 and 92.52% by 10 μM DhHP-6).

Furthermore, the inhibitory effect of DhHP-6 on fibril formation was measured by western blot analysis. In all samples, $A\beta_{1-42}$ self-assembled into monomers, oligomers (trimers and tetramers, 14–18 kDa) and large oligomers (~100 kDa, Fig. 3). DhHP-6 significantly reduced the aggregation of large oligomers (Fig. 3A) and oligomers (trimers and tetramers, Fig. 3B), while slightly increasing monomer levels (Fig. 3C).

The supra-molecular structure of $A\beta_{1-42}$ fibrils in the presence of DhHP-6 was analysed using TEM. Non-fibrillar Aβ (stored at 4 °C for 5 days) formed nanometre-sized spherical particles, along with areas of special thinner and shorter fibrils (Fig. 4A). A fibrillar network was detected in pure $A\beta_{1-42}$ that was incubated at 37 °C for 5 days (Fig. 4B). In comparison, a striking reduction of fibrillation, spherical aggregates, and smaller diameters could be found in samples with DhHP-6 added (Fig. 4C). The results demonstrate the substantial inhibition of $A\beta_{1-42}$ aggregation by DhHP-6.

3.2. Affinity of DhHP-6 for $A\beta_{1-42}$ assessed by BLI

Affinity of DhHP-6 for $A\beta_{1-42}$ was examined with the BLI system. DhHP-6 rapidly bound and dissociated from Aβ (immobilised on the chip surface) with a dissociation constant (K_D) of 100 ± 12 μM (Fig. 5A). The K_D of the β-sheet breaker (LPFFD, positive control) was 350 ± 47 μM (Fig. 5B, Table S1) [28]. Thus, DhHP-6 has a much higher affinity for Aβ than LPFFD, indicating that DhHP-6 strongly binds Aβ.

3.3. DhHP-6 reduces the percentage of β-sheets in $A\beta_{1-42}$

Based on the preceding results, we surmised that DhHP-6 might inhibit Aβ aggregation by changing its secondary structure. The effect of DhHP-6 on the conformational changes in $A\beta_{1-42}$ were assessed by CD spectrometry. Pure $A\beta_{1-42}$ and DhHP-6 mixed with $A\beta_{1-42}$ were assessed at 0 and 72 h. The initial secondary structure of $A\beta_{1-42}$ was less α-helical, composed mainly of β-sheets and random coils with a strong CD signal at 197 nm (Fig. 6A). After a 72-h incubation with DhHP-6, there remained only a weak CD signal at approximately 197 nm, clearly indicating that DhHP-6 reduced β-sheet structures (Fig. 6B). The percentage of β-sheets was reduced from 89.1% to 78.3% by DhHP-6 (Table 1).

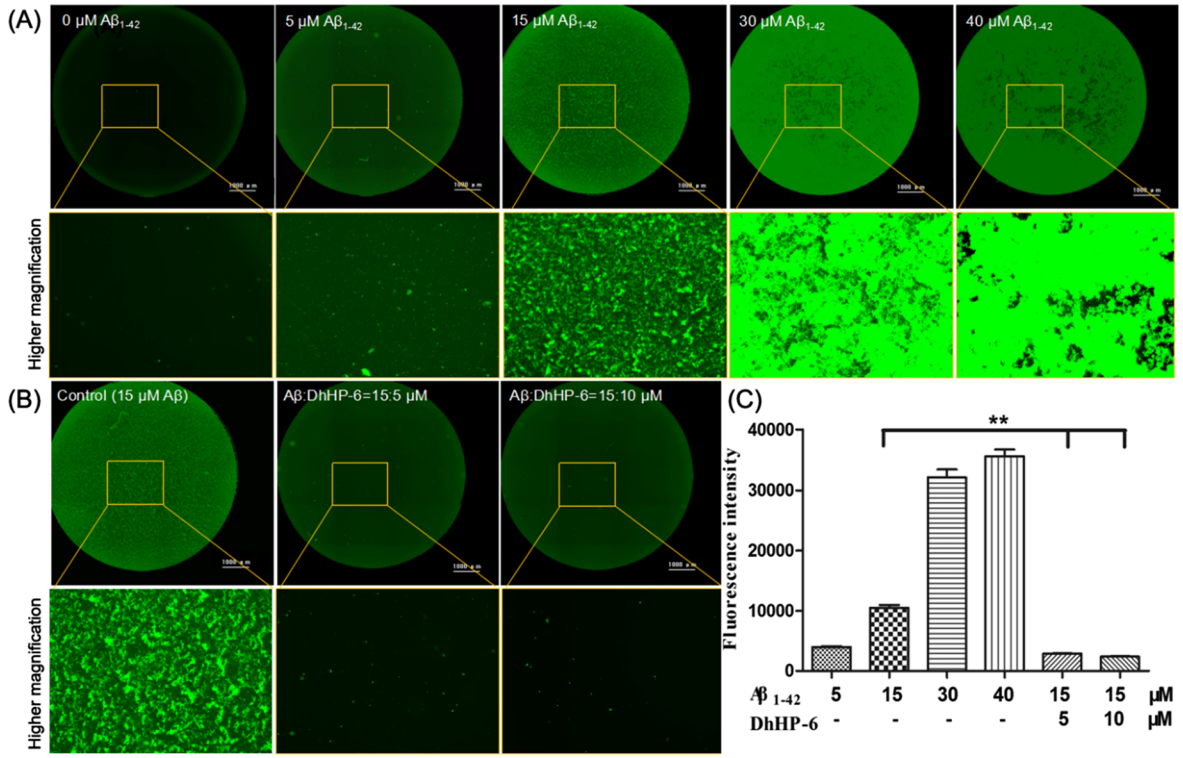

Fig. 2. DhHP-6 reduced the aggregation of $A\beta_{1-42}$ *in vitro*, as assessed with the Cell Imaging Multi-Mode Reader. (A) The aggregation of $A\beta_{1-42}$ at initial concentrations of 0 to 40 μM were photographed. (B) DhHP-6 significantly reduces the aggregation of $A\beta_{1-42}$ *in vitro* in a dose-dependent manner. The inhibition ratio of $A\beta_{1-42}$ is 72.62% (5 μM DhHP-6), and 92.52% (10 μM DhHP-6). An enlarged view shows that DhHP-6 reduces the formation of fibrils significantly. (C) The fluorescence intensities in Fig. 2A and B were measured with a cell imaging multi-mode reader. The bars represent the mean ± SD, $^{**}p < 0.01$.

3.4. DhHP-6 binds Aβ closely, as revealed by molecular docking analysis

To provide additional insight into the interaction between DhHP-6 and $A\beta_{1-42}$, molecular docking simulations were performed. A study [31] showed that two stretches of hydrophobic residues (16–20 and 30–40), as well as His, Glu, Asp, and Lys, play important roles in the process of $A\beta_{1-42}$ aggregation via hydrophobic and electrostatic interactions. The final simulated configurations of docking of DhHP-6 with $A\beta_{1-42}$ are shown in Fig. 7. DhHP-6 bound to $A\beta_{1-42}$ at the α-helix and β-sheet structures. This complex was stabilised by two intermolecular hydrogen bonds between DhHP-6 and Glu^{11}:OE2/Glu^{22}:OE1, a intermolecular electrostatic bond (pi–pi) at DhHP-6(Fe)–Aβ(Phe^4) and four intermolecular hydrophobic bonds at DhHP-6(C)–Aβ(Val^{18}) (pi–pi), Aβ(Phe^4)–DhHP-6(C), Aβ(His^{14})–DhHP-6(C), and DhHP-6 with Aβ at Arg^5 (pi–alkyl). Additionally, a pi–anion bond was found at DhHP-6(Fe)–Aβ (Phe^4) and an alkyl bond at Aβ(His^{14})–DhHP-6(C). Notably, the proposed interaction of DhHP-6 and $A\beta_{1-42}$ occurs predominantly between amino acids in the β-sheet structures, which likely inhibit the misfolding and aggregation of $A\beta_{1-42}$.

3.5. DhHP-6 significantly extends lifespan, alleviates Aβ-induced paralysis and reduces the aggregation of $A\beta_{1-42}$ in CL4176 transgenic worms

C. elegans strain CL4176, which produces low levels of $A\beta_{1-42}$ even when grown at 25 °C, was chosen to evaluate the potential protective effects of DhHP-6 *in vivo*. In our previous study, 100 μM DhHP-6 was the optimal concentration for *C. elegans*-based assays [19,20]. Here, we found that 100 μM DhHP-6 significantly extended survival of CL4176 at 25 °C (Fig. 8A). Furthermore, the percentage of paralysed worms was significantly reduced by DhHP-6 (100 μM), by 33.33% and 61.94% on days 4 and 5, respectively, compared with the control group (Fig. 8B). These findings suggest that DhHP-6 reduces Aβ-induced toxicity in strain CL4176, thereby alleviating paralysis and extending lifespan. The effect of DhHP-6 on $A\beta_{1-42}$ aggregation in CL4176 was also evaluated by ThT staining. Worms treated with DhHP-6 (100 μM) were nearly completely free of light spots (representing $A\beta_{1-42}$ aggregations, Fig. 8C). Quantification of the ThT fluorescence (Fig. 8D) with Image software demonstrated that DhHP-6 significantly reduced $A\beta_{1-42}$ aggregation in CL4176 transgenic worms compared with the control group. These results indicate that DhHP-6 alleviates paralysis by reducing $A\beta_{1-42}$ plaques in the nematode.

4. Discussion

It is generally agreed that the massive deposition of misfolded protein aggregates is the key for elucidating the pathological mechanism and features underlying AD. Self-assembled oligomers and Aβ protofibrils, but not monomeric Aβ, exhibit toxicity to neuronal cells. Therefore, any strategy that interferes with or inhibits Aβ aggregation at the very early stage may reduce Aβ toxicity, which represents a valid approach for prevention of neuronal degeneration and protection against AD. Several small molecules [24,25], short peptides [26,27,32–34], chemicals [35,36], chaperone proteins, and nanoparticles [31,37] exhibit interaction with or inhibition of the Aβ self-assembly process; however, their safety, stability and economic benefits are still key problems that affect their application. Recently, short peptides have been a focus for the design of inhibitors of Aβ aggregation. Tjernberg [38] proposed that the inhibitor KLVFF ($A\beta_{16-20}$) recognises and binds to full-length Aβ, inhibiting the aggregation of monomeric Aβ into fibrils that are the key core for forming the β-sheet structure. The pentapeptide inhibitor LPFFD, designed based on the LVFF ($A\beta_{17-20}$) sequence, is well-known as a "β-sheet breaker" (BSB) that inhibits Aβ fibrillogenesis and prevents neuronal degeneration [39]. Also, some short peptides were designed to target the key hydrophobic core region of β-amyloid by electrostatic interaction, hydrogen bonds or hydrophobic interaction. However, to date no one has

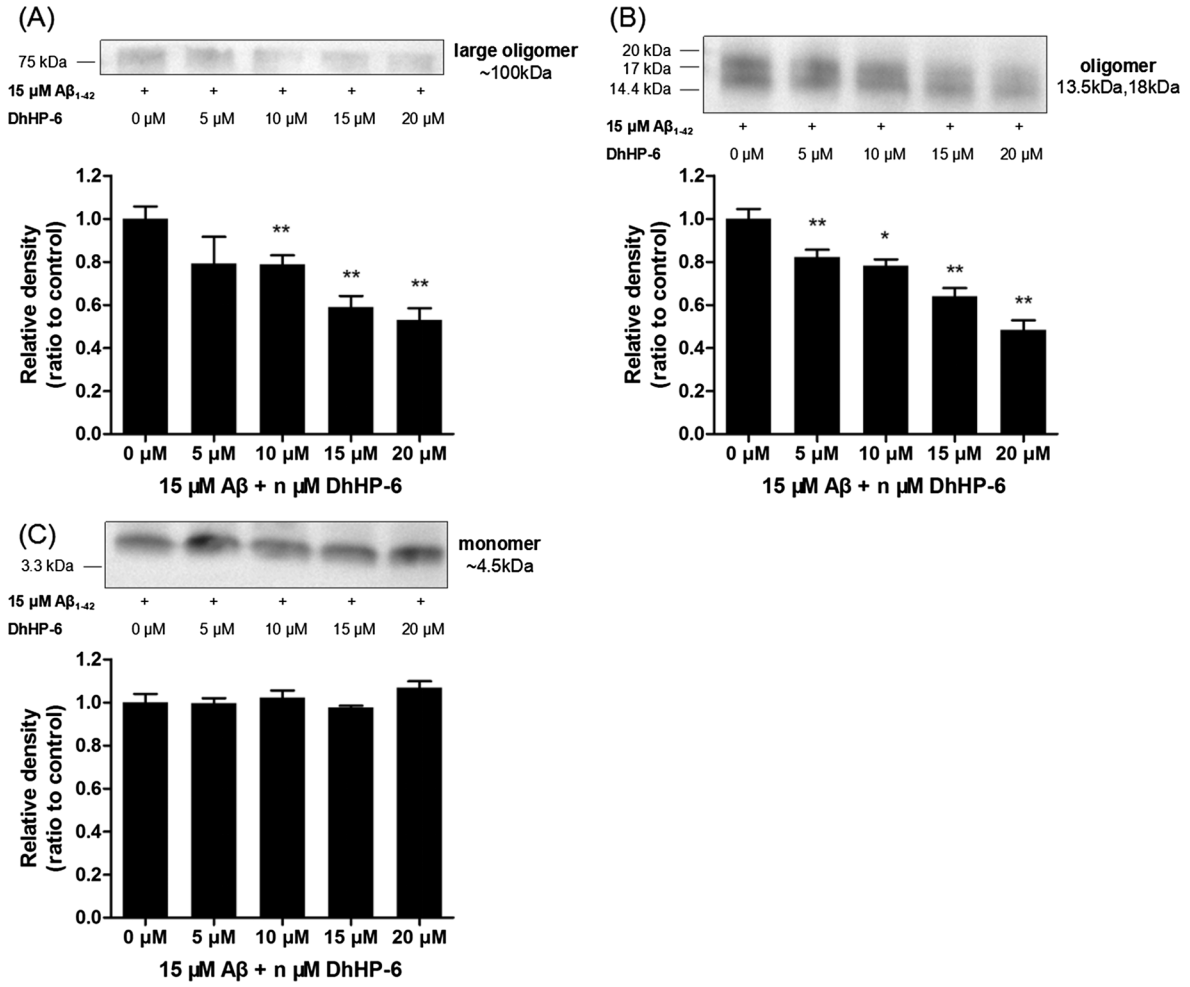

Fig. 3. DhHP-6 significantly reduced the formation of $A\beta_{1-42}$ aggregates by western blot analysis. (A) Compared with pure Aβ, 10, 15 and 20 μM DhHP-6 reduced the relative grey value of large oligomers by 21, 41 and 47%, respectively. (B) Compared with pure Aβ, 5, 10, 15 and 20 μM DhHP-6 reduced the relative grey value of oligomers by 18, 22, 36 and 52%, respectively. (C) The relative grey value of monomers in Fig. 3C. The entire blot was shown in Fig. S2. $A\beta_{1-42}$ was mixed with DhHP-6 (0, 5, 10, 15 or 20 μM) and incubated at 37 °C for 24 h, and then subjected to western blot analysis. The bars represent the mean ± SD, and three times of independent experiments, $^{*}p < 0.05$, $^{**}p < 0.01$.

chosen the natural peroxidase, MP-11, as a model to design a peroxidase mimic that has excellent antioxidant activity and inhibits β-amyloid fibrillogenesis.

DhHP-6, as a heme peptide derivative, was designed based on the catalytic site structure of MP-11 [40]. DhHP-6 contains covalent-binding type deuterohemin and polypeptides with histidine. DhHP-6 exhibits outstanding water solubility, stability and is easier to synthesise compared with MP-11. As an artificial microperoxidase mimic, DhHP-6 scavenges hydroxyl free radicals at ~94% that of MP-11, which makes it an excellent antioxidant, especially for oxidative stress-related diseases such as ageing [18]. This prompted us to infer that DhHP-6 could serve as an alternative drug for the treatment of AD

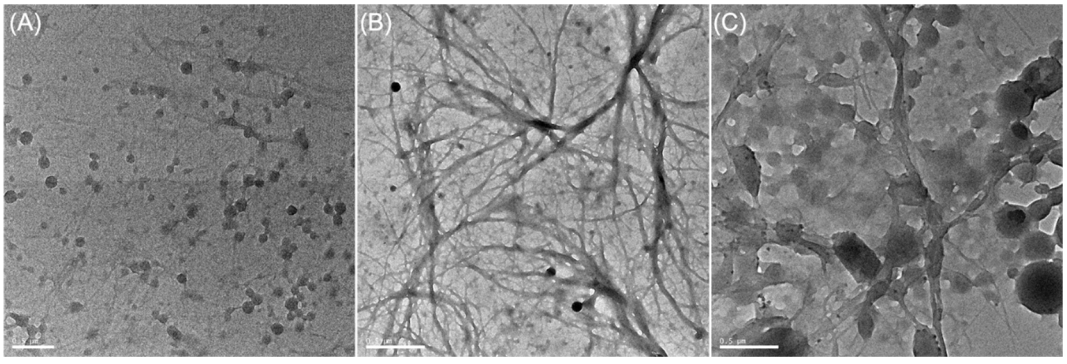

Fig. 4. The supra-molecular structure of $A\beta_{1-42}$ fibrils in the presence of DhHP-6 was analysed using TEM. (A) Non-fibrillar Aβ (stored at 4 °C for 5 days) formed nanometre-sized spherical particles, along with areas of special thinner and shorter fibrils. (B) A fibrillar network was detected in pure $A\beta_{1-42}$ that was incubated at 37 °C for 5 days. (C) A striking reduction of fibrillation, spherical aggregates, and smaller diameters could be found in samples with DhHP-6 added. Scale bar = 0.5 μm.

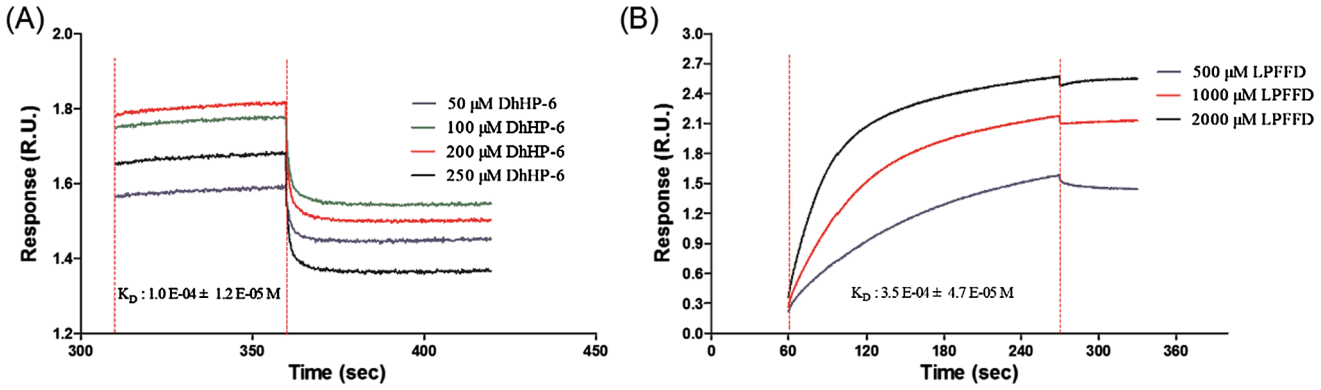

Fig. 5. Affinity of DhHP-6 for $A\beta_{1-42}$ was examined with the BLI system. (A) DhHP-6 rapidly bound and dissociated from Aβ (immobilised on the chip surface) with a dissociation constant (K_D) of 100 ± 12 μM. (B) The K_D of the β-sheet breaker (LPFFD, positive control) was 350 ± 47 μM. Various concentrations of DhHP-6 and the short peptide LPFFD was injected for 50 s at a flow rate of 30 μL/min, followed by a 70 s dissociation phase. The chip was regenerated with 50 mM sodium hydroxide and sodium dodecyl sulfonate (SDS) solution.

because of its antioxidant activity and because the special deuterohemin peptide with the ferric porphyrin structure binds with Aβ.

In this study, the quantitative ThT fluorescence assay showed that the aggregation of Aβ was time- and dose-dependent. ThT fluorescence reduced significantly by adding different molar ratios of DhHP-6, indicating that DhHP-6 delayed or inhibited the aggregation of Aβ. The reaction time was fast but the mechanism is not yet clear. Based on these results, we surmise that DhHP-6 may bind to Aβ to form Aβ/DhHP-6 complexes or change the secondary structure of Aβ, thereby reducing Aβ aggregation. Western blot results verified that DhHP-6 significantly reduced the content of oligomers (trimers and tetramers) and larger aggregates, with no significant effects on monomers. TEM further validated that DhHP-6 reduced the formation of dense fibrillar networks to spherical particles, likely by maintaining Aβ in the large oligomeric state with less fibres. Preliminary results showed DhHP-6 inhibited Aβ aggregation at the early filamentous stage.

At the same time, the BLI system was used to evaluate the affinity of DhHP-6 with $A\beta_{1-42}$. Compared with the β-sheet breaker, LPFFD (350 ± 47 μM), DhHP-6 exhibited a stronger binding affinity with rapid binding and dissociation (K_D = 100 ± 12 μM), reflecting the multiple weak bonding interactions. These results further explained the western blot results, indicating that DhHP-6 could bind with Aβ monomer to form proper steric hindrance, which blocked the formation of oligomers and larger aggregates by interfering with Aβ self-aggregation. In addition, the transformation of Aβ secondary structural upon addition of DhHP-6 was evaluated by CD spectroscopy. After a 72-h incubation, the peak at approximately 197 nm was clearly reduced, and the percentage of β-sheets was reduced from 89.1% to 78.3%.

Table 1
β-sheet percentage of $A\beta_{1-42}$ was reduced by DhHP-6.

		α-Helix	β-Sheet	Random coil	β-Sheet percentage
0 h	Aβ	12.6	58.7	28.7	
	Aβ + DhHP-6	14.8	52.3	32.9	89.1
72 h	Aβ	2.8	75.2	22.0	
	Aβ + DhHP-6	12.3	58.9	28.8	78.3

These results reflected that DhHP-6 disrupts β-sheets, which play an important role in Aβ aggregation and fibril formation. Both the BLI and CD assays revealed that DhHP-6 bound closely with Aβ, and β-sheet sites may also be target binding sites. Molecular docking simulated the molecular interactions between DhHP-6 and Aβ. Phe^4, Glu^{11}, His^{14}, Val^{18} and Glu^{22} sites in the α-helix and β-sheets had important effects on binding and interactions due to ionic and hydrogen bonds or hydrophobic interactions. Further, the ferric centre of the porphyrin structure had a close integration with Aβ at Phe^4 with a Pi-Pi shape and Pi-anion. Collectively, the findings strongly suggested that DhHP-6 primarily and strongly binds with Aβ monomers at β-sheets to hinder the self-aggregation of Aβ to form large oligomers or fibres *in vitro*.

Furthermore, DhHP-6 (100 μM) significantly increased the longevity and alleviated the paralysis of *C. elegans* strain CL4176 by reducing the β amyloid-induced aggregation and toxicity. This indicated that DhHP-6 also effectively reduces or delays the formation of amyloid plaques *in vivo*. However, the molecular mechanisms by which DhHP-6 protects worms *in vivo*, whether by antioxidant activity as a peroxidase mimic and/or as an inhibitor that binds to and changes the secondary

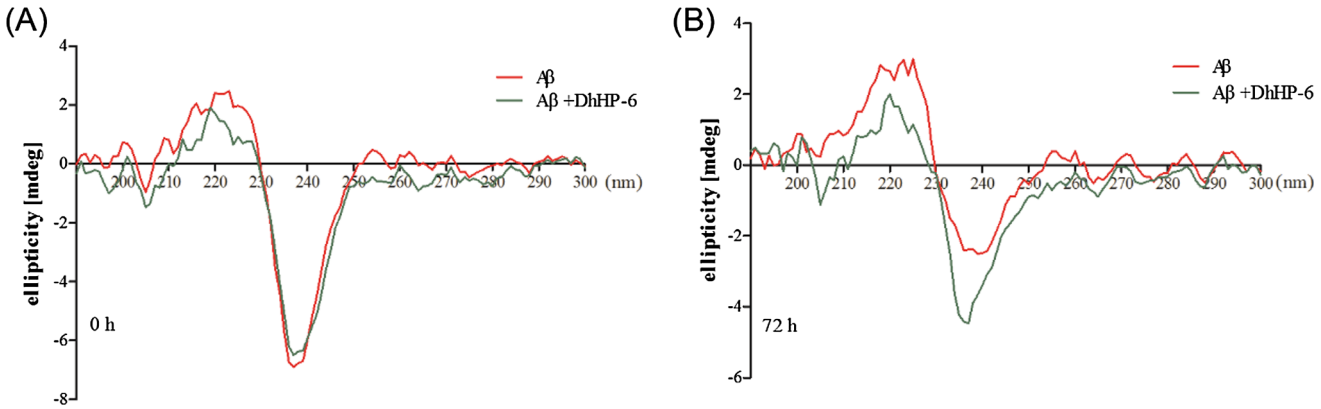

Fig. 6. Effect of DhHP-6 on the conformational changes in $A\beta_{1-42}$ were assessed by CD spectrometry. Pure $A\beta_{1-42}$ and $A\beta_{1-42}$ mixed with DhHP-6 (75:25 mol ratio) in PB buffer (pH 7.4) were assessed at (A) 0 h and (B) 72 h. Secondary structure values were estimated by spectral deconvolution (refer to Table 1).

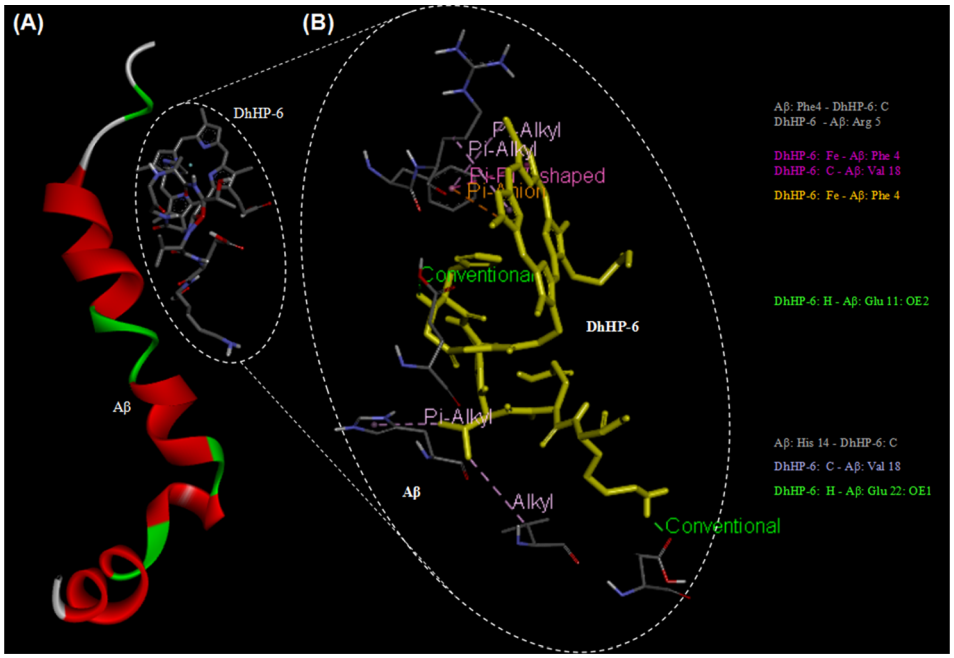

Fig. 7. Molecular docking model of DhHP-6 binding to the $A\beta_{1-42}$ monomer. (A) The simulated relative position of DhHP-6 molecule bound to $A\beta_{1-42}$. (B) The DhHP-6 molecule was bound to $A\beta_{1-42}$ via two intermolecular hydrogen bonds between DhHP-6 and $Glu^{11/22}$, an intermolecular electrostatic bond at DhHP-6(Fe)–Aβ(Phe^4) and four intermolecular hydrophobic bonds at DhHP-6(C)–Aβ(Val^{18}) (pi–pi), Aβ(Phe^4)–DhHP-6(C), Aβ(His^{14})–DhHP-6(C) and DhHP-6–Aβ(Arg^5) (pi–alkyl). Also, a pi–anion bond can be found at DhHP-6(Fe)–Aβ(Phe^4) and an alkyl bond at Aβ(His^{14})–DhHP-6(C).

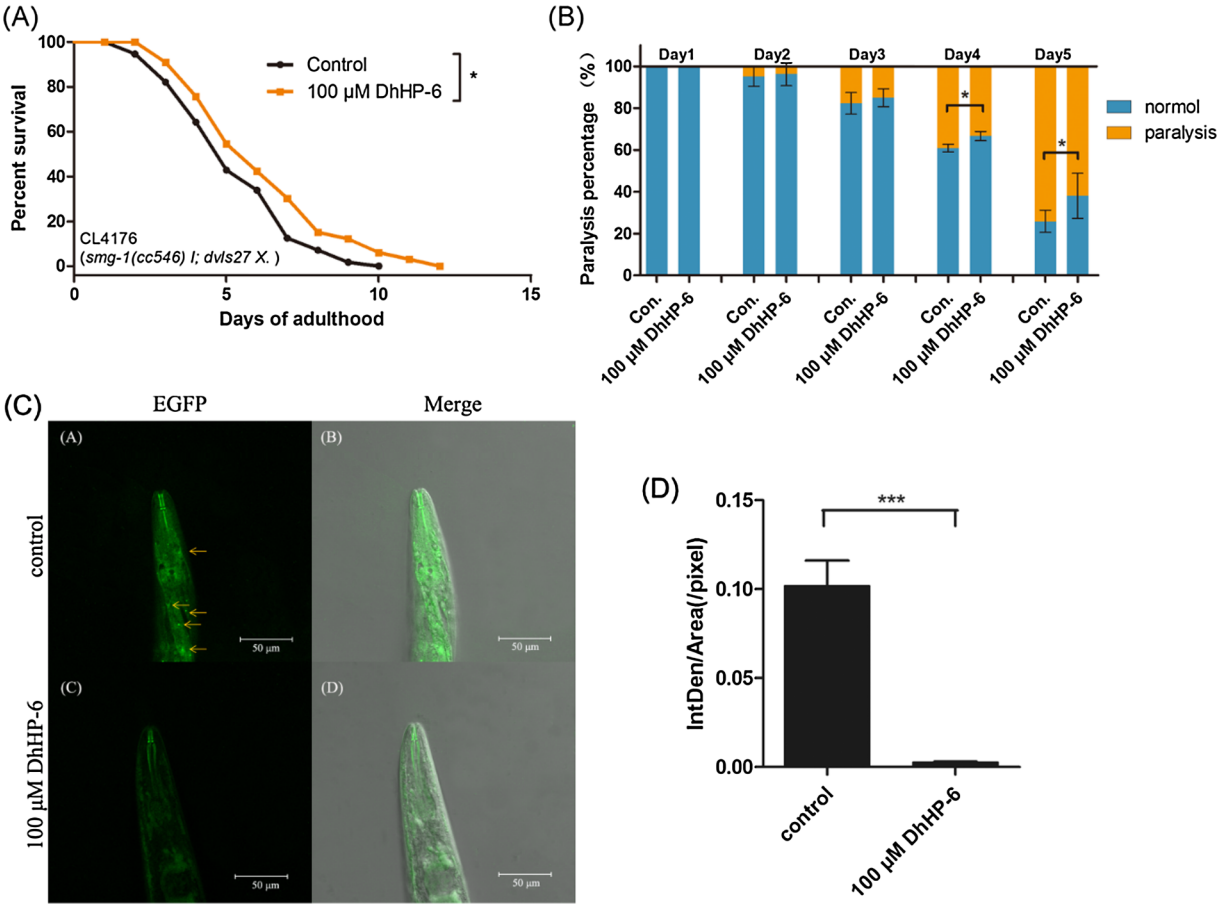

Fig. 8. DhHP-6 significantly extended lifespan, alleviated $A\beta_{1-42}$-induced paralysis and reduced $A\beta_{1-42}$ aggregation in CL4176 transgenic worms. (A) DhHP-6 significantly extended survival of CL4176 at 25 °C ($^{*}p < 0.05$). (B) 100 μM DhHP-6 alleviates the Aβ-induced paralysis of CL4176 at 25 °C, by 33.33% and 61.94% on days 4 and 5, respectively ($^{*}p < 0.05$). (C) DhHP-6 significantly reduced $A\beta_{1-42}$ aggregation in CL4176 transgenic worms by ThT staining assay. Worms treated with DhHP-6 (100 μM) were nearly completely free of light spots. (D) ThT fluorescence intensity was quantified in the control and DhHP-6 groups by Image software, $^{***}p < 0.001$. All experiments were performed three times, and the bars represent the mean ± SD.

structure of β amyloid, are not yet clear. Further *C. elegans* and Alzheimer's transgenic mice (APPswe/PSEN1dE9) experiments are being carried out. We speculate that DhHP-6 has therapeutic potential for the treatment of AD and may serve as a bifunctional alternative drug that shows antioxidant activity and inhibition of Aβ aggregation.

Acknowledgment

This study was supported by grants from the National Natural Science Foundation of China, China (No. 31401086), Jilin Province Science and Technology Development Program, China (No. 20150520157JH) and the China Postdoctoral Science Foundation Grant, China (No. 2015M581398). We thank Ann Turnley, PhD, from Liwen Bianji, Edanz Group China (www.liwenbianji.cn/ac), for editing the English text of a draft of this manuscript.

Author contributions

Conceived and designed the experiments: J.X., L.P.W., performed the experiments: J.X., Y.Y., R.N.Z., Y.H.S., T.Z.S., analyzed the data: J.X., Y.Y., R.N.Z., J.Q.W., contributed reagents/materials/analysis tools: C.H.W., Y.J.C., contributed to the writing of the manuscript: J.X., S.W.G., L.P.W. All authors agree with the presented findings, and that the work has not been published before.

Competing financial interests

The authors declare no competing financial interests.

Ethical approval and informed consent

All animal studies were conducted in accordance with legal and institutional guidelines. The procedures were approved by the Ethical Committee of Care and Use of Laboratory Animals at Jilin University.

Appendix A. Supplementary material

Supplementary data to this article can be found online at https://doi.org/10.1016/j.bioorg.2018.10.072.

References

[1] A. Francioso, P. Punzi, A. Boffi, C. Lori, S. Martire, C. Giordano, M. D'Erme, L. Mosca, beta-sheet interfering molecules acting against beta-amyloid aggregation and fibrillogenesis, Bioorg. Med. Chem. 23 (2015) 1671–1683.
[2] H.J. Möller, M.B. Graeber, The case described by Alois Alzheimer in 1911, Eur. Arch. Psychiatry Clin. Neurosci. 248 (1998) 111–122.
[3] J. Gaugler, B. James, T. Johnson, K. Scholz, J. Weuve, Alzheimer's disease facts and figures, Alzheimers Dementia 12 (2016) (2016) 459–509.
[4] M. Awasthi, S. Singh, V.P. Pandey, U.N. Dwivedi, Alzheimer's disease: An overview of amyloid beta dependent pathogenesis and its therapeutic implications along with in silico approaches emphasizing the role of natural products, J. Neurol. Sci. 361 (2016) 256–271.
[5] K. Blennow, H. Hampel, CSF markers for incipient Alzheimer's disease, Lancet Neurol. 2 (2003) 605–613.
[6] H. Hampel, R. Frank, K. Broich, S.J. Teipel, R.G. Katz, J. Hardy, K. Herholz, A.L. Bokde, F. Jessen, Y.C. Hoessler, Biomarkers for Alzheimer's disease: academic, industry and regulatory perspectives, Nat. Rev. Drug Discovery 9 (2010) 560.
[7] S.H. Omar, C.J. Scott, A.S. Hamlin, H.K. Obied, The protective role of plant biophenols in mechanisms of Alzheimer's disease, J. Nutr. Biochem. 47 (2017) 1–20.
[8] C. Haass, A.Y. Hung, D.J. Selkoe, Processing of beta-amyloid precursor protein in microglia and astrocytes favors an internal localization over constitutive secretion, J. Neurosci. 11 (1991) 3783–3793.
[9] J.A. Hardy, G.A. Higgins, Alzheimer's disease: the amyloid cascade hypothesis, Science (New York, N.Y.) 256 (1992) 184–185.
[10] K. Hsiao, P. Chapman, S. Nilsen, C. Eckman, Y. Harigaya, S. Younkin, F. Yang, G. Cole, Correlative memory deficits, Aβ elevation, and amyloid plaques in transgenic mice, Science (New York, N.Y.) 274 (1996) 99–102.
[11] J. Näslund, V. Haroutunian, R. Mohs, K.L. Davis, P. Davies, P. Greengard, J.D. Buxbaum, Correlation between elevated levels of amyloid β-peptide in the brain and cognitive decline, JAMA 283 (2000) 1571–1577.
[12] W.L. Klein, W.B.S. Jr, D.B. Teplow, Small assemblies of unmodified amyloid β-protein are the proximate neurotoxin in Alzheimer's disease, Neurobiol. Aging 25 (2004) 569–580.
[13] J. Hardy, D.J. Selkoe, The amyloid hypothesis of Alzheimer's disease: progress and problems on the road to therapeutics, Science (New York, N.Y.) 297 (2002) 353–356.
[14] G.P. Morris, I.A. Clark, B. Vissel, Inconsistencies and controversies surrounding the amyloid hypothesis of Alzheimer's disease, Acta Neuropathol. Commun. 2 (2014) 135 2,1(2014-09-18).
[15] K.D. Jacob, H.N. Noren, T. Tadokoro, A. Lohani, J. Barnes, M.K. Evans, Alzheimer's disease-associated polymorphisms in human OGG1 alter catalytic activity and sensitize cells to DNA damage, Free Radical Biol. Med. 63 (2013) 115–125.
[16] M.A. Smith, X. Zhu, M. Tabaton, G. Liu, M.K.D. Jr, M.L. Cohen, X. Wang, S.L. Siedlak, B.E. Dwyer, T. Hayashi, Increased iron and free radical generation in preclinical Alzheimer disease and mild cognitive impairment, J. Alzheimers Dis. Jad 19 (2010) 363.
[17] Y.L. Liu, L. Guo, R. Roeske, G.M. Luo, L.I. Wei, The method improvement of synthyesis and purification of deuterohemin, Acta Scientiarium Naturalium Universitatis Jilinensis (2001).
[18] L.P. Wang, Y.L. Liu, H. Yang, L.I. Wei, Synthesis and anti-cataract activity of a novel peroxidase mimetics, Chem. Res. Chin. Univ. 25 (2004) 2171–2173.
[19] S. Guan, P. Li, J. Luo, Y. Li, L. Huang, G. Wang, L. Zhu, H. Fan, W. Li, L. Wang, A deuterohemin peptide extends lifespan and increases stress resistance in Caenorhabditis elegans, Free Radical Res. 44 (2010) 813–820.
[20] L. Huang, P. Li, G. Wang, S. Guan, X. Sun, L. Wang, DhHP-6 extends lifespan of Caenorhabditis elegans by enhancing nuclear translocation and transcriptional activity of DAF-16, Free Radical Res. 47 (2013) 316–324.
[21] G. Mccoll, B.R. Roberts, A.P. Gunn, K.A. Perez, D.J. Tew, C.L. Masters, K.J. Barnham, R.A. Cherny, A.I. Bush, The caenorhabditis elegans Aβ1–42 model of alzheimer disease predominantly expresses Aβ3–42, J. Biol. Chem. 284 (2009) 22697–22702.
[22] Z. Zhang, H. Ma, X. Wang, Z. Zhao, Y. Zhang, B. Zhao, Y. Guo, L. Xu, A tetrapeptide from maize protects a transgenic Caenorhabditis elegans Aβ1-42 model from Aβ-induced toxicity, Rsc Adv. 6 (2016).
[23] V. Fonte, D.R. Kipp, Y.J. Rd, D. Merin, M. Forrestal, E. Wagner, C.M. Roberts, C.D. Link, Suppression of in vivo beta-amyloid peptide toxicity by overexpression of the HSP-16.2 small chaperone protein, J. Biol. Chem. 283 (2008) 784–791.
[24] K. Rajasekhar, K. Mehta, T. Govindaraju, Hybrid multifunctional modulators inhibit multifaceted abeta toxicity and prevent mitochondrial damage, ACS Chem. Neurosci. 9 (2018) 1432–1440.
[25] D. Mendes, M.M. Oliveira, P.I. Moreira, J. Coutinho, F.M. Nunes, D.M. Pereira, P. Valentao, P.B. Andrade, R.A. Videira, Beneficial effects of white wine polyphenols-enriched diet on Alzheimer's disease-like pathology, J. Nutr. Biochem. 55 (2018) 165–177.
[26] B.M. Austen, K.E. Paleologou, S.A. Ali, M.M. Qureshi, D. Allsop, O.M. Elagnaf, Designing peptide inhibitors for oligomerization and toxicity of Alzheimer's beta-amyloid peptide, Biochemistry 47 (2008) 1984–1992.
[27] C. Wasmer, A. Lange, H.V. Melckebeke, A.B. Siemer, R. Riek, B.H. Meier, Amyloid fibrils of the HET-s(218-289) prion form a β solenoid with a triangular hydrophobic core, Science (New York, N.Y.) 319 (2008) 1523–1526.
[28] J. Liu, W. Wang, Q. Zhang, S. Zhang, Z. Yuan, Study on the efficiency and interaction mechanism of a decapeptide inhibitor of beta-amyloid aggregation, Biomacromolecules 15 (2014) 931–939.
[29] H. LeVine 3rd, J.D. Scholten, Screening for pharmacologic inhibitors of amyloid fibril formation, Methods Enzymol. 309 (1999) 467–476.
[30] M.R. Nilsson, Techniques to study amyloid fibril formation in vitro, Methods 34 (2004) 151–160.
[31] Y. Liu, L.P. Xu, W. Dai, H. Dong, Y. Wen, X. Zhang, Graphene quantum dots for the inhibition of β amyloid aggregation, Nanoscale 7 (2015) 19060.
[32] M.H. Baig, K. Ahmad, G. Rabbani, I. Choi, Use of peptides for the management of Alzheimer's disease: diagnosis and inhibition, Front. Aging Neurosci. 10 (2018).
[33] S. Liu, S. Park, G. Allington, F. Prelli, Y. Sun, M. Martá-Ariza, H. Scholtzova, G. Biswas, B. Brown, P.B. Verghese, Targeting apolipoprotein E/amyloid β binding by peptoid CPO_Aβ17-21 P ameliorates Alzheimer's disease related pathology and cognitive decline, Sci. Rep. 7 (2017) 8009.
[34] Q. Zhang, J. Liu, X. Hu, W. Wang, Z. Yuan, In vitro studies on accelerating the degradation and clearance of amyloid-β fibrils by an antiamyloidogenic peptide, Acs Macro Lett. 4 (2015) 339–342.
[35] Z. Lin, T. Chi, X. Zhao, Y. Lei, S. Song, Q. Lu, X. Ji, L. Peng, L. Wang, L. Zou, Xanthoceraside modulates neurogenesis to ameliorate cognitive impairment in APP/PS1 transgenic mice, J. Physiol. Sci. (2017) 1–11.
[36] G. Sun, J. Wang, X. Guo, M. Lei, Y. Zhang, X. Wang, X. Shen, L. Hu, Design, synthesis and biological evaluation of LX2343 derivatives as neuroprotective agents for the treatment of Alzheimer's disease, Eur. J. Med. Chem. 145 (2018) 622–633.
[37] S. Xiao, D. Zhou, P. Luan, B. Gu, L. Feng, S. Fan, W. Liao, W. Fang, L. Yang, E. Tao, R. Guo, J. Liu, Graphene quantum dots conjugated neuroprotective peptide improve learning and memory capability, Biomaterials 106 (2016) 98–110.
[38] L.O. Tjernberg, C. Lilliehook, D.J. Callaway, J. Naslund, S. Hahne, J. Thyberg, L. Terenius, C. Nordstedt, Controlling amyloid beta-peptide fibril formation with protease-stable ligands, J. Biol. Chem. 272 (1997) 12601–12605.
[39] C. Soto, E.M. Sigurdsson, L. Morelli, R.A. Kumar, E.M. Castano, B. Frangione, Beta-sheet breaker peptides inhibit fibrillogenesis in a rat brain model of amyloidosis: implications for Alzheimer's therapy, Nat. Med. 4 (1998) 822–826.
[40] A. Spector, W. Zhou, W. Ma, C.F. Chignell, K.J. Reszka, Investigation of the mechanism of action of microperoxidase-11, (MP11), a potential anti-cataract agent, with hydrogen peroxide and ascorbate, Exp. Eye Res. 71 (2000) 183–194.